

Influences of surface contaminating elements on potential-induced degradation of crystalline silicon solar cells



Yiming Qin ^{a,*}, Asahi Yonemoto ^a, Marwan Dhamrin ^b, Keisuke Ohdaira ^c, Kazuhiro Gotoh ^{a,d}, Atsushi Masuda ^{a,d}

^a Graduate School of Science and Technology, Niigata University, Japan

^b Graduate School of Engineering, Osaka University, Japan

^c Japan Advanced Institute of Science and Technology, Japan

^d Interdisciplinary Research Center for Carbon-Neutral Technologies, Niigata University, Japan

ARTICLE INFO

Keywords:

Crystalline Si solar cell
Photovoltaic modules
Potential-induced degradation
Alkali metal elements

ABSTRACT

Effects of alkali metal on the potential-induced degradation (PID) phenomena in wafer-based conventional p-type crystalline silicon technologies were studied. It is known that sodium rapidly and severely brings the shunting-type PID (PID-s) phenomenon; however, the impact of other alkali metal such as lithium and potassium on the PID-s phenomenon is unrevealed. We used solar cells that light-receiving surface was contaminated with lithium, sodium or potassium, and in order to control the sodium content, prepared were photovoltaic modules without cover glass and performed were PID tests and anneal tests. During the tests, the performance of each module was judged by the current-voltage measurements and the electroluminescence images. After a certain time of PID tests, the secondary ion mass spectrometry analysis was performed on the solar cells of some modules. Thus, the penetration status of alkali metal elements is judged. From the PID tests and anneal tests, we conclude that, the negative potential of the solar cell light-receiving surface is the basis of the PID-s phenomenon. Furthermore, in the PID tests, all elements penetrated into the solar cell, but only sodium rapidly causes severe PID-s phenomenon. The PID-s phenomenon appears to be moderated when both lithium and sodium are present on the solar cell light-receiving surface. Therefore, we believe that lithium and potassium do not cause PID-s phenomenon, and lithium seems to mitigate the sodium-induced PID-s phenomenon.

1. Introduction

In response to global energy depletion, photovoltaic (PV) technology is one of the renewable energy technologies currently being developed owing to the outstanding advantages of low manufacturing and maintenance costs and a long service life. However, some degradation phenomena occurring during the outdoor operation of PV modules can reduce their photon-electron conversion efficiency. Potential-induced degradation (PID) phenomena of crystalline silicon (c-Si) solar cells, which is due to a high potential difference between the solar cell and other parts of the module (glass, mount or aluminum (Al) frame), is a major degradation mechanism. To date, PID has been intensively studied since its discovery and the phenomenon has been recognized as a challenge to the reliability of PV modules including c-Si solar cells [1–3]. Nowadays, in mainstream operating PV systems, the voltage difference between the external metal frame of the module and the solar cells

reaches hundreds of volts or even more, which facilitates the PID phenomena, resulting in considerable short-term power generation losses. In particular, shunting-type PID (PID-s) phenomenon has been reported to cause significant power losses in PV modules during operation and are most common in existing PV systems [4,5]. According to several studies, PID-s phenomenon is caused by stacking faults formed by the penetration of sodium (Na) in the cover glass or on the solar cell light-receiving surface into the interior of c-Si [6–12]; which enhances recombination processes in the solar cell. The recombination processes are considered to be caused by recombination in the depletion region because of Na-decorated stacking faults, leading to an increase in the saturation current density (J_{02}) of the second diode [13]. At the same time, Na penetration leads to a decrease in the solar cell shunt resistance (R_{sh}) [14]. Meanwhile, there have been several reports that PID is a key attenuation mechanism not only in the p-type c-Si solar cells, but also on the backside of bifacial passivated emitter and rear cells (PERC⁺)

* Corresponding author. Graduate School of Science and Technology, Niigata University, 8050, Ikarashi 2-no-cho, Nishi-ku, Niigata 950-2181, Japan.
E-mail address: f24l004a@mail.cc.niigata-u.ac.jp (Y. Qin).

[15–21]. Na invasion leads to an initial PID (n^+ layer), and as Na continues to invade to the point of crossing the pn junction to the p-layer it leads to an irreversible PID. In all Si solar cells, the intrusion of Na leads to an initial PID (n^+ layer) with a concomitant decrease in open-circuit voltage (V_{oc}) and R_{sh} ; as Na continues to intrude into the pn junction, it produces a stacking layer and further increases the recombination, leading to a further decrease in V_{oc} and R_{sh} ; and as Na passes through the pn junction to reach the p-layer, the V_{oc} and R_{sh} decrease dramatically, and an irreversible PID is caused at the same time.

Soda-lime cover glass is widely used in current mainstream PV modules and is the main Na source causing the PID-s. The common soda-lime glass is composed of 14 mass% Na_2O , 0.01 mass% Li_2O and 0.03 mass% K_2O , indicating alkali metal elements other than Na (such as potassium (K) elements [22]) coexist in the common soda-lime cover glass. These alkali metal elements are currently difficult to be removed in a low-cost manner. The influence of these alkali metal elements on the PID-s phenomenon has not been studied in detail. Since these homologous elements have similar physical and chemical properties, we hypothesized that Li or K element could also cause a PID-s phenomenon similar to Na element. To verify this hypothesis, we performed PID experiments using deliberately contaminated mono c-Si solar cells with different alkali metal elements.

2. Experimental methods

2.1. Module fabrication

In the conventional PV module shown in Fig. 1a, a large amount of Na element and other alkali metal elements are present in the common soda-lime cover glass adhered to the solar cell light-receiving surface by

the encapsulant material, so that the amounts of the Na element and other contaminant alkali metal elements are uncontrollable during the PID tests. On the other hand, when non-alkaline glass is used, most of the voltage in the PID-s phenomenon is applied to the non-alkaline glass because its resistivity is much higher than that of the encapsulant. The use of non-alkaline glass makes it difficult to reproduce the same PID-s phenomenon as that observed in modules fabricated using the soda-lime cover glass. Therefore, in this study, preliminary tests were conducted to search for an optimum module structure that can generate the PID-s phenomenon with the c-Si solar cells contaminated by the controlled amount of alkali metal elements.

As shown in Fig. 1, the optimum module structure was searched by three steps of modifications to the conventional module. In step 1, the structure without the cover glass on the solar cell light-receiving surface in the PV module (Fig. 1a to b) was examined. Since there is no way to know the total amount of alkali elements in the cover glass, quantitative evaluation of the elements affecting the PID-s phenomenon cannot be performed. Hence, the PID test should be performed by the PV module without using the soda-lime cover glass. However, when such PV modules were laminated, the encapsulating material (e.g. ethylene-vinyl acetate (EVA) copolymer) became soft. Due to the absence of the soda-lime cover glass, the interconnectors soldered to silver (Ag)-electrodes on the c-Si solar cell light-receiving surface changed the shape of the EVA and the EVA on the interconnectors became thinner. This reduced the distance between the interconnector and the Al tape attached to the EVA surface as the electrode for the PID test, causing a short-circuit in some cases. Next, in step 2, two sheets of encapsulant materials were employed on the solar cell light-receiving surface in the PV module (Fig. 1b to c). As shown in Fig. 1c, one EVA sheet was added to ensure the distance between the interconnector and the Al tape on the solar cell

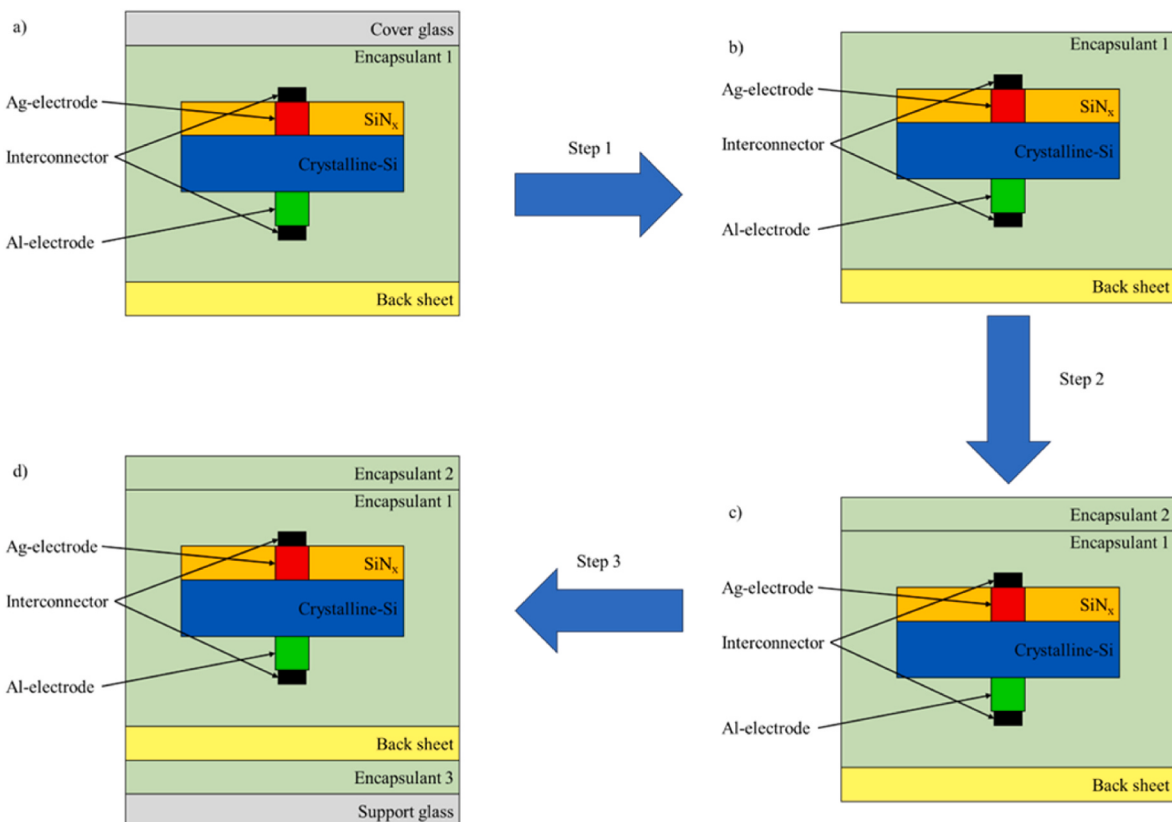


Fig. 1. Conceptual drawings of a cross-section of the proposed optimized processes for the module without the cover glass based on the conventional PV module. The conventional PV module a), the module without the cover glass b), the module without the cover glass with the additional encapsulant 2 on the solar cell light-receiving surface c), and the module without the cover glass with the additional encapsulant 2 on the solar cell light-receiving surface, and the encapsulant 3 and the support glass both on the back side of the back sheet d).

light-receiving surface. However, since most of the strength of the PV module is maintained by the cover glass, the mechanical strength of the PV module shown in Fig. 1c was weak due to the absence of the cover glass on the solar cell light-receiving surface. The c-Si solar cells in such PV modules were prone to cracking due to manipulation during PID testing. Next, in step 3, as shown in Fig. 1d, both encapsulant material and support glass were added on the back side of the back sheet surface of the PV module (Fig. 1c to d). As shown in Fig. 1d, the cover glass on the solar cell light-receiving surface was moved to the back side of the back sheet surface as support glass to maintain the mechanical strength of the PV module without affecting the solar cell light-receiving surface, which is essential for the PID-s phenomenon. For the module-level PID tests [23], the voltage is applied between the shorted interconnector of the solar cell and the Al plate or the Al tape attached to the outside of the cover glass on the solar cell light-receiving surface. Therefore, the addition of the support glass and EVA for adhering the glass to the outside of the back sheet does not affect the PID test results. After the preliminary tests described above, it was decided to carry out a PID test on the module with the structure shown in Fig. 1d.

2.2. Contamination source

In this study, the light-receiving surface of the c-Si solar cells was intentionally contaminated with the alkali metal elements before being modularized. The contamination source used in this study was prepared by mixing a fixed amount of each alkali metal chloride powder with ultrapure water (H_2O) as solutions of different concentrations in the measuring flask. The purity of the alkali metal chloride powder used in this study was 99.5 % for lithium chloride (LiCl), 99.95 % for both sodium chloride (NaCl) and potassium chloride (KCl). Almost all impurity components in each type of the alkali metal chloride powder are other alkali metals other than the main components. The alkali chloride aqueous solutions were dropped onto the center of the c-Si solar cell light-receiving surface as contamination sources: LiCl aqueous solution (LiCl [H_2O]), NaCl aqueous solution (NaCl [H_2O]), and KCl aqueous solution (KCl [H_2O]). Then, the solar cell was placed in air at an ambient temperature of 25 °C for 16 h or longer to ensure complete evaporation of the water in the solution.

Among ionic compounds containing the alkali metal element, the best option is the alkali metal halide. The alkali metal cations in the alkali metal halide ionic compounds on the c-Si solar cell light-receiving surface are supposed to migrate into the cell interior due to the electric field and temperature during the PID test. On the other hand, the halogen anions are thought to move in the opposite direction of the electric field, i.e. towards the encapsulant, where they react with the small amount of water vapor remaining in the encapsulant during their migration and form the hydrogen halide molecules. The halogens here are fluorine (F), chlorine (Cl), bromine (Br) or iodine (I). In this study, Cl compounds were selected for the contamination source. In general, Cl anion, which is non-toxic, non-polluting and the most stable in the PID test environment. Furthermore, hydrogen chloride generated from chloride compounds does not chemically react with silicon nitride (SiN_x) for the anti-reflection coating of c-Si solar cells. Jonai et al. reported that PID-s can be caused by the contamination method using chloride crystals [9]. Therefore, alkaline metal chloride solutions were used in this study based on the previous reports.

2.3. PID tests

In this study, commercially available conventional Al back surface field (Al BSF) p-type c-Si solar cells ($156 \times 156 \text{ mm}^2$), which are susceptible to PID phenomena, were selected for the experiments and cleaved into several small $30 \times 30 \text{ mm}^2$ mini-cells.

After soldering the interconnectors to the miniature c-Si solar cells, 0.1 ml of the alkali metal chloride aqueous solution with different concentrations was dropped onto the c-Si solar cell light-receiving

surface as the contamination source. The types and concentrations of the contamination sources dropped are listed in Table 1. As a control, a module with a cell only dropping H_2O was also fabricated.

The modules were fabricated using three sheets of 450 μm thick encapsulant (EVA) and 326 μm thick back sheet, and support glass (Asahi Glass Co., Ltd., 210,716-F8). The volume resistivity of the EVA encapsulant is larger than $2 \times 10^{15} \Omega \text{ cm}$. The back sheet consists of three layers of 38 μm thick polyvinyl fluoride (PVF), 250 μm thick polyethylene terephthalate (PET) and 38 μm thick PVF. As a contrast, a conventional module using cover glass without cell contamination was also made. The specification of the cover glass is the same as the support glass. Ten modules with an external size of $45 \times 45 \text{ mm}^2$ were fabricated by vacuum lamination according to the stacking sequence shown in Fig. 1d. The thickness of the EVA encapsulants 1, 2 and 3 are all the same 450 μm . The vacuum lamination sequence and conditions were vacuum evacuation (3 min), vacuum pressing (10 min) and vacuum keeping (5 min) at 150 °C. Depending on the contamination source and test conditions, each module is labeled L1-L3, N1-N3, K1-K3 and H as shown in Table 1.

The PID tests were carried out on all the modules fabricated using the methods described. Since EVA softens when the PID tests were conducted under temperature conditions exceeding 65 °C the environmental conditions during the PID tests were also set at a temperature of 65 °C, and relative humidity (RH) of 2 % or less in this test. In the PID test, as shown in Fig. 2, the EVA surface on the solar cell light-receiving surface was grounded by attaching Al tape as a positive electrode. The two interconnectors were shorted as a negative electrode, and the DC voltage of 1000 V was applied between them. According to these conditions, the PID tests were carried out simultaneously on seven PV modules in total: L1-L2, N1-N2, K1-K2, and H modules. The L3, N3, and K3 modules were exposed to an ambient temperature of 65 °C and RH of 2 % or less to verify the effect of only heating without voltage application. This test is referred to as the anneal test in this paper.

The current-voltage (*I-V*) characteristics of each PV module were measured before and after the PID test or the anneal test using the two light-source solar simulator with xenon and halogen lamps. The *I-V* measurements were carried out under standard test conditions (STC) according to IEC 61853-1 at a measurement temperature of 25 °C (± 1 °C), air mass (AM) of 1.5 and irradiation intensity of 100 mW/cm². It was confirmed that initial values of short-circuit current density (J_{sc}), V_{oc} , and fill factor (FF) show small derivation and the typical values were 33.0 mA/cm², 0.59 V, 0.78 respectively. Electroluminescence (EL) images were also evaluated using an EL imaging system. In addition, the secondary ion mass spectrometry (SIMS) was performed on the cells to check whether each alkali metal element penetrates the cell after the PID test. The SIMS measurement area was approximately 1 cm² on one side separated by the interconnector soldered to the c-Si solar cell. The measurement depth from the solar cell surface was 3 μm .

Table 1
Module IDs, the contamination source solution types and the solution concentrations, and applied voltage for the PID and anneal tests.

Module ID	Contamination source solution type	Solution concentration (mol/L)	Applied voltage (V)	Total test duration (h)
L1	LiCl [H_2O]	0.02	1000	96
L2	LiCl [H_2O]	0.2	1000	96
L3	LiCl [H_2O]	0.2	0	96
N1	NaCl [H_2O]	0.02	1000	96
N2	NaCl [H_2O]	0.002	1000	19
N3	NaCl [H_2O]	0.02	0	96
K1	KCl [H_2O]	0.02	1000	96
K2	KCl [H_2O]	2	1000	72
K3	KCl [H_2O]	2	0	96
H	H_2O	–	1000	72

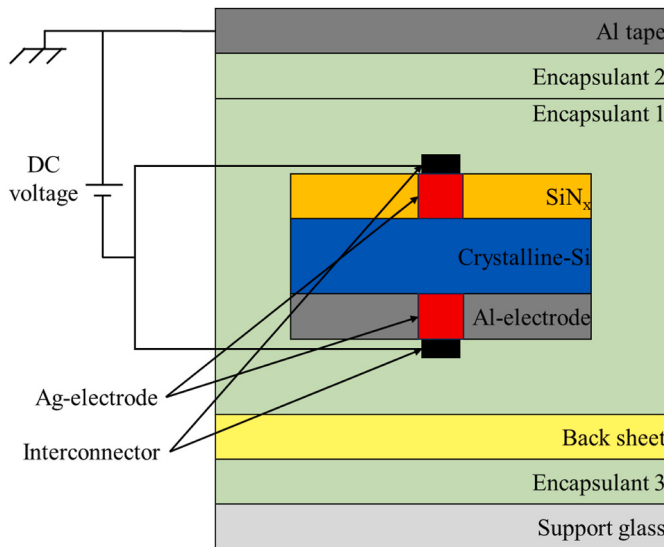


Fig. 2. Conceptual drawing of a cross-section of the PID test using the PV module without the cover glass shown in Fig. 1d.

3. Results and discussion

Figs. 3–6 show V_{oc} , R_{sh} , FF, and power conversion efficiency (PCE) as a function of the PID test duration or the anneal test duration. The parameters are normalized by the respective initial value after the lamination for each module. From Fig. 3a–6a, V_{oc} , R_{sh} , FF, and PCE of N1 and N2 modules show a significant decrease (over than 10 %) due to the PID test. V_{oc} , R_{sh} , FF, and PCE of the other modules show a slight decrease

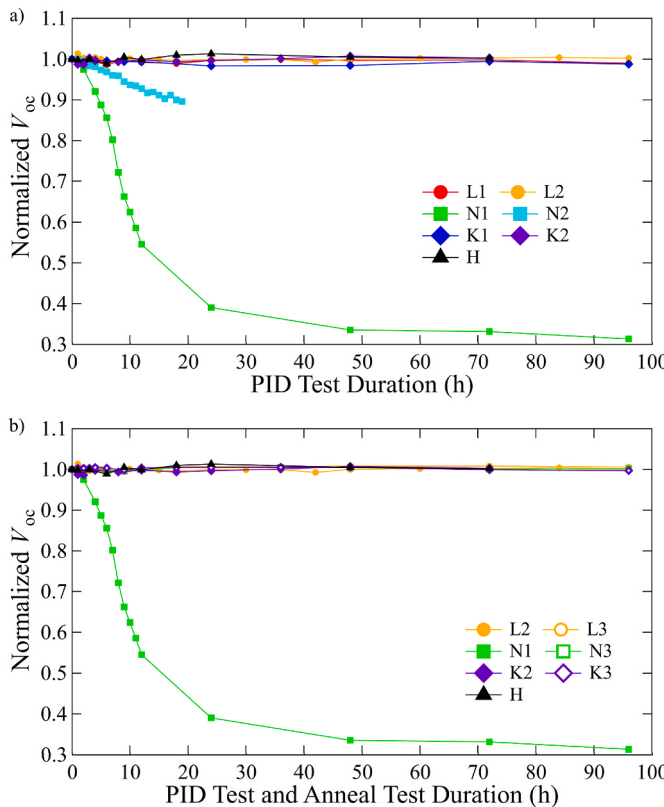


Fig. 3. Normalized V_{oc} as a function of PID test duration (a), and PID and anneal test duration (b) for L1-L3, N1-N3, K1-K3 and H modules. Lines are guides to the eye.

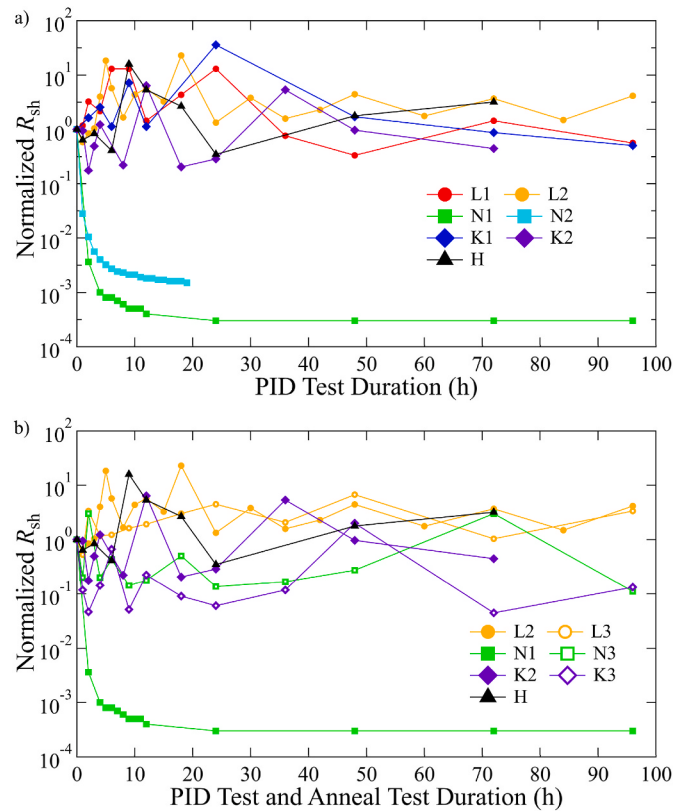


Fig. 4. Normalized R_{sh} as a function of PID test duration (a), and PID and anneal test duration (b) for L1-L3, N1-N3, K1-K3 and H modules. Lines are guides to the eye.

(less than 10 %); however, the amount of decrease is negligible compared to N1 and N2 modules. Furthermore, it can be seen that a decrease in each I-V parameter of the N1 module is larger than that of the N2 module. This indicates that the higher the amount of Na element contamination results in larger decrease in the performance of the solar cell. As shown in Fig. 3b–6b, V_{oc} , R_{sh} , FF, and PCE of L3, N3 and K3 modules remain almost unchanged. There is almost no degradation of the solar cell performance when no voltage is applied to the solar cell, indicating that the application of voltage is a key to cause a decrease in the performance of the solar cell. Furthermore, the annealing temperature of 65°C is not enough to cause Na diffusion into the interior of the solar cell [24]. Surprisingly, as shown in Fig. 6a, the PID test on the modules with the solar cells contaminated by alkali metal elements other than the Na element shows that the performance degradation is much smaller.

As shown in Fig. 7, during the module-level PID test using the conventional module with the cover glass, the PCE decreases to less than 5 % of the initial value as the PID test duration increases. That is, Na in the cover glass gradually penetrated into the solar cell with the electric field until the c-Si solar cell is completely degraded. However, in the test shown in Fig. 6a, after 24 h of PID test, the PCE of the N1 module drops to about 10 % of the initial value, and the PCE hardly continues to drop after 96 h of PID test. In other words, it has reached the saturation state. This means that the Na ions on the solar cell light-receiving surface in the N1 module have almost completely penetrated into the c-Si solar cell. It has been estimated that even if all the Na ions in 0.1 ml of 0.02 mol/L NaCl (H_2O) (about 1.2×10^{18} atoms) penetrated into the solar cell, it would not be enough to completely degrade the c-Si solar cell of about $3 \times 3 \text{ cm}^2$. Meanwhile, as shown in Fig. 6a, after the 20 h of PID test, the PCE of the N2 module decreased to about 40 % of the initial value, which is much smaller than that of the N1 module (which decreased to about 15 % or less of the initial value). This indicates that

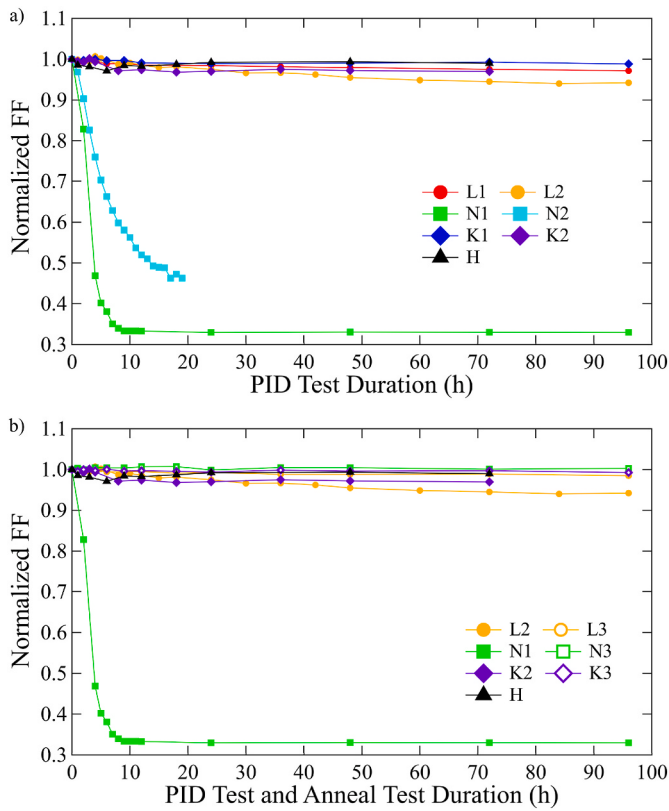


Fig. 5. Normalized FF as a function of PID test duration (a), and PID and anneal test duration (b) for L1-L3, N1-N3, K1-K3 and H modules. Lines are guides to the eye.

the concentration of Na ions present on the solar cell light-receiving surface affects the rate of decline in the performance of the module and the magnitude of the decline.

As shown in Fig. 4a, a decrease in R_{sh} of the N1 and N2 modules, i.e. the Na-contaminated c-Si solar cells, was onset just after the PID test. Furthermore, as the PID test progresses, the R_{sh} of the N1 module continues to decrease and saturates at about 24 h. Moreover, R_{sh} drops significantly immediately after the start of the PID test and dominates the decrease in PCE. On the other hand, such a decreasing trend of R_{sh} was not observed for the L1-3 and K1-3 modules from Fig. 4, and thus the PCE of these modules hardly decreased as shown in Fig. 6. This result suggests that a decrease in PCE of the modules due to PID testing is due to a decrease in R_{sh} of the modules. It was reported that the incorporation of Na elements into the Si crystal results in the formation of stacking faults and modification of the Na elements inside the crystalline Si [25]. The presence of stacking faults and the modification of Na decreases R_{sh} and increases recombination in the depletion layer region, which increases J_{02} .

As shown in Fig. 5a and 6a, a decreasing trend of FF for all modules is similar to that of PCE. It is clear from Fig. 4a and 5a that the decline in FF follows the decline in R_{sh} . This indicates that a decrease in R_{sh} is the main reason for a decrease in FF. This is consistent with the typical PID-s phenomenon.

As shown in Fig. 3a and 6a, a decrease in V_{oc} was remarkable for the N1 and N2 modules compared with other modules. This means that V_{oc} significantly decreased only when the solar cell surface was contaminated with Na and voltage was applied. The V_{oc} values of other modules are almost identical after the PID test or the anneal test. As shown in Fig. 3a and 6a, when contaminated by the Na element, the decrease rate in V_{oc} is related to a decrease rate in PCE; however, after the first 2 h of the PID test, PCE decreases to about 80 % of the initial value, but V_{oc} does not decrease much. As the PID test continues, V_{oc} decreases rapidly.

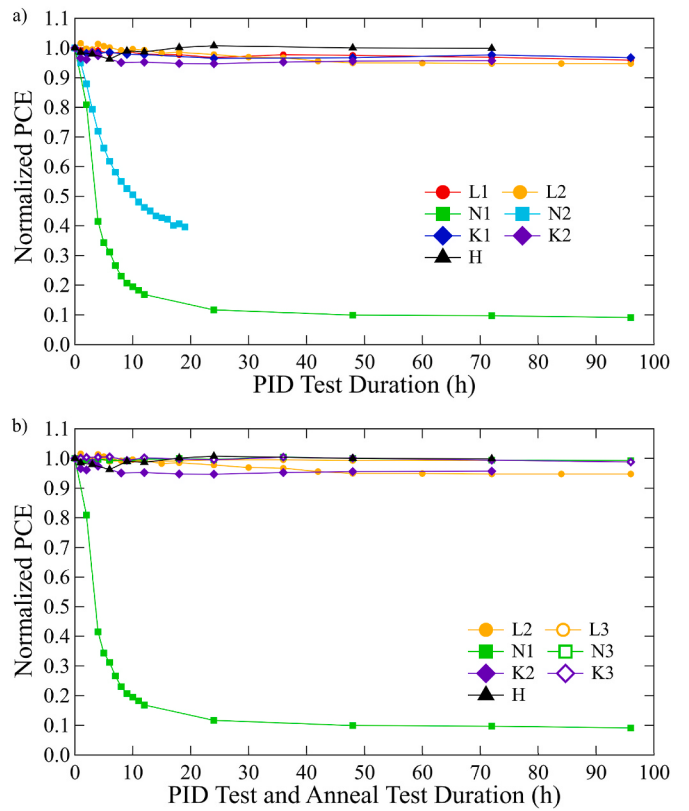


Fig. 6. Normalized PCE as a function of PID test duration (a), and PID and anneal test duration (b) for L1-L3, N1-N3, K1-K3 and H modules. Lines are guides to the eye.

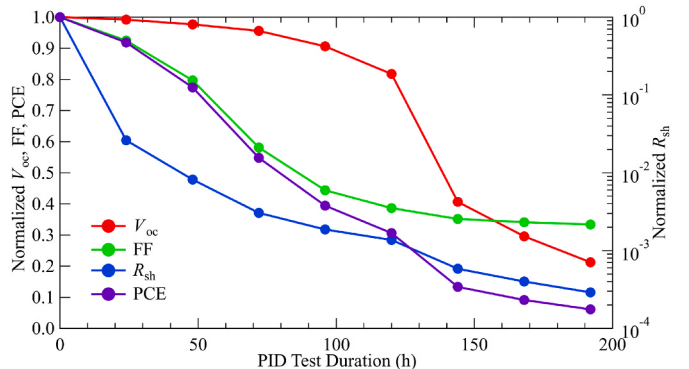


Fig. 7. Normalized V_{oc} , FF, R_{sh} , and PCE as a function of PID test duration for the conventional module. Lines are guides to the eye.

The V_{oc} reduction can be primarily explained by R_{sh} reduction. Furthermore, it is reported that PID causes an increase in n_2 and J_{02} , which also reduce V_{oc} . In the early stages of the PID-s phenomenon, the Na element may not penetrate deeply into the pn junction of the crystalline Si solar cell, so their effect on V_{oc} may be slight. As the PID test duration increases, the Na element penetrates deeper into the pn junction and forms a large number of stacking faults [26], which may damage the Si crystal structure, causing an increase in the second diode ideality factor (n_2) and J_{02} , which may result in a significant decrease in V_{oc} [26–28]. Even if all the Na atoms on the solar cell surface penetrate the solar cell, it is assumed that the damage to the structure of c-Si depends on the total amount of Na and the penetration depth.

From Figs. 3–6, it can be seen that the parameters (including V_{oc} , R_{sh} , FF, PCE) of H module are almost unchanged until the PID test for 72 h.

This indicates that when the solar cell light-receiving surface is free of contamination, the PID-s phenomenon does not occur even if the module is subjected to under temperature at 65 °C and applied voltage of DC 1000 V.

In addition, Fig. 8 shows EL images taken before and after the PID or the anneal test for all the modules. From Fig. 8, it can be seen that the EL images of N1 and N2 modules were not observed after the PID test. This is due to the PID-s phenomenon occurring in N1 and N2 modules. On the other hand, the EL images of the other modules are almost free of dark areas except for those due to cracking before the PID tests, which is consistent with the solar cell parameters shown in Figs. 3–6, indicating that the PID-s phenomenon does not occur in these modules. The EL image of the L1 module became slightly dark after the PID test. This suggests that impurities, mainly NaCl, in LiCl cause a slight PID-s phenomenon. However, no notable dark area was observed for the EL image of the L2 module contaminated with an even denser concentration of the LiCl [H₂O] after the PID test. This indicates that the EL images do not darken when more Li elements are present on the solar cell light-receiving surface even though contaminated with more Na elements. The EL images of the cells contaminated with K also show no change

after the PID test, regardless of the K concentration. This suggests that the much lower content of impurities (mainly NaCl) in KCl do not reach the minimum Na content required for the occurrence of the PID phenomenon. In addition, the EL images of the H module do not change before and after the PID tests. These phenomena are consistent with the I-V measurement results.

To explain the above experimental results, we hypothesized that in PV modules using c-Si solar cells contaminated with elemental Li or K on the light-receiving surface, either 1) PID-s will not occur due to Li or K inaccessibility in the solar cell, or 2) PID-s will be negligible even if Li or K penetrates the solar cell, and we tried to experimentally clarify the correctness of the following two hypotheses. The first hypothesis is that the PID-s phenomenon does not occur because the Li element or the K element does not penetrate the c-Si solar cell during the PID test. The second hypothesis is that Li or K element does not cause the PID-s phenomenon even if Li or K element penetrates the c-Si solar cell by the PID test. To clarify the above two hypotheses, SIMS measurements were performed after PID testing in a module with cells contaminated with high concentrations of the aqueous solution of alkali metal elements and H₂O, i.e. the L2, N1, K2 (contaminated with highly

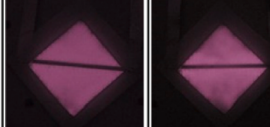
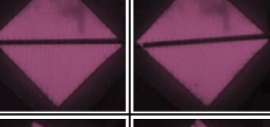
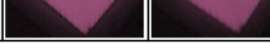
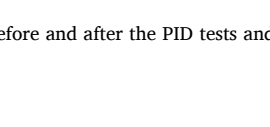
Module ID	Test time (h)	PID test		Module ID	Test time (h)	Anneal test	
		Before PID test	After PID test			Before PID test	After PID test
L1	96						
L2	96			L3	96		
N1	96			N3	96		
N2	19						
K1	96						
K2	72			K3	96		
H	72						

Fig. 8. EL images before and after the PID tests and the anneal test of L1-L3, N1-N3, K1-K3, and H modules.

concentrated solutions), and H modules.

The Li, Na, K concentrations measured by SIMS are shown in Fig. 9. The elements depth profiles of modules contaminated with LiCl, NaCl, KCl, and H₂O solutions are shown in Fig. 9a, 9b, 9c, and 9d, respectively. The thickness of the SiN_x layer was about 80 nm and the pn junction is located about 400 nm deep from the solar cell surface. From Fig. 9a–c, it is clear that all the alkali metal elements can pass through the SiN_x layer of the solar cell and penetrate the pn junction during the PID test regardless of the type of contamination source. Note that the depth resolution is lower because it is sputtered from a textured surface. As shown in Fig. 9d, all the alkali metal elements are also detected in the solar cells with drops of H₂O; however, the amount is very small in comparison with those for other modules and does not affect the PID-s phenomenon. In other words, even if a small amount of alkali metal elements (Li [not more than 3×10^{16} atom/cm³], Na [not more than 6×10^{15} atom/cm³], K [not more than 7×10^{16} atom/cm³]) penetrates the c-Si solar cell, the PID-s phenomenon may not occur.

As mentioned above, the performance of the N1 module is significantly degraded after the PID test. As shown in Fig. 9b, SIMS results show that the Na elements of the order of 6.3×10^{18} atom/cm³ pass through not only the SiN_x but also the pn junction (about 0.4 μm) and penetrate the c-Si solar cell, significantly reducing the performance of the c-Si solar cell. As shown in Figs. 3–6, the amount of performance degradation of the L2 module after 96 h of the PID test is negligible compared to the N1 module; the performance degradation after 72 h of the PID test for the K2 module and the H module is also negligible. It is assumed that the amount of permeation of the Na element in modules other than N1 and N2 modules is less than the amount considered to cause PID phenomena, resulting in smaller performance degradation. As shown in Fig. 9a and b, comparing the penetration depth and amount of Na element between the L2 and N1 modules, the difference in Na element concentration is about 10 times at a depth of 0.5 μm from the solar cell light-receiving surface; however, there is no significant degradation in I-V characteristics of the L2 module, even with the PID test. As shown in Fig. 9a, 9c, and 9d, the penetration depth and amount of Na element for the K2 module or the H module is even smaller than for the L2 module, and there is no degradation in the power generation performance. On the other hand, the I-V characteristics of the N1 module

are significantly reduced by the PID test. Furthermore, as shown in Fig. 9a–c, comparing the depth and amount of Na element penetration into each module, the N1 module is the largest, followed by the L2 module with the K2 module, while the H module is the smallest. This suggests that the slight PID-s phenomenon that occurs when contaminated with Li or K element can be attributed to NaCl impurities in the LiCl or KCl.

In the L2 module, the performance degradation due to the PID-s phenomenon is slight compared to the N1 module, despite the fact that the Na element penetrates about 0.1 times more than in the N1 module. This suggests that Li element may have the effect of mitigating the performance degradation of the PID-s phenomenon caused by Na element. As shown in Fig. 9a and 9b, comparing the penetration depth and penetration amount of Li element in the L2 and N1 modules, the amount of Li element at a depth of 0.5 μm from the solar cell light-receiving surface is about 1000 times larger for the L2 module than for the N1 module. Therefore, the SIMS analyses revealed that hypothesis 2 of the two hypotheses presented above may be correct. That is, Li element or K element does not cause the PID-s phenomenon even if such element penetrates the solar cell by the PID test.

We found that the PID phenomenon is very sensitive to Na contamination, but insensitive to Li and K contamination. The origin of the different effects of different alkali metals on the PID phenomenon is not clear. The impact of impurity on semiconductors is generally dependent on the amount of incorporated impurity and the position of impurity levels in the bandgap. It is known that the ionic radius of Li, Na and K are 60, 95 and 133 pm respectively [29]. The diffusion of the Li, Na, K ions is expected to be different since the ionic radii of the elements are different, however the concentrations of Li for L2, of Na for N1 and of K for K2 at pn-junction are almost same level. This suggests the degradation was not affected by the amount of the incorporated elements, but by the position of an energy level of the Li, Na and K in bandgap. Although Na and K form relatively deep donor levels, Li forms a shallow donor level [30]. This can be explained by the small effect of Li atoms on the PID-s phenomenon, but not by the effect of K atoms. Therefore, further study is necessary to clarify the origin of the different effects of different alkali metals on the PID phenomenon.

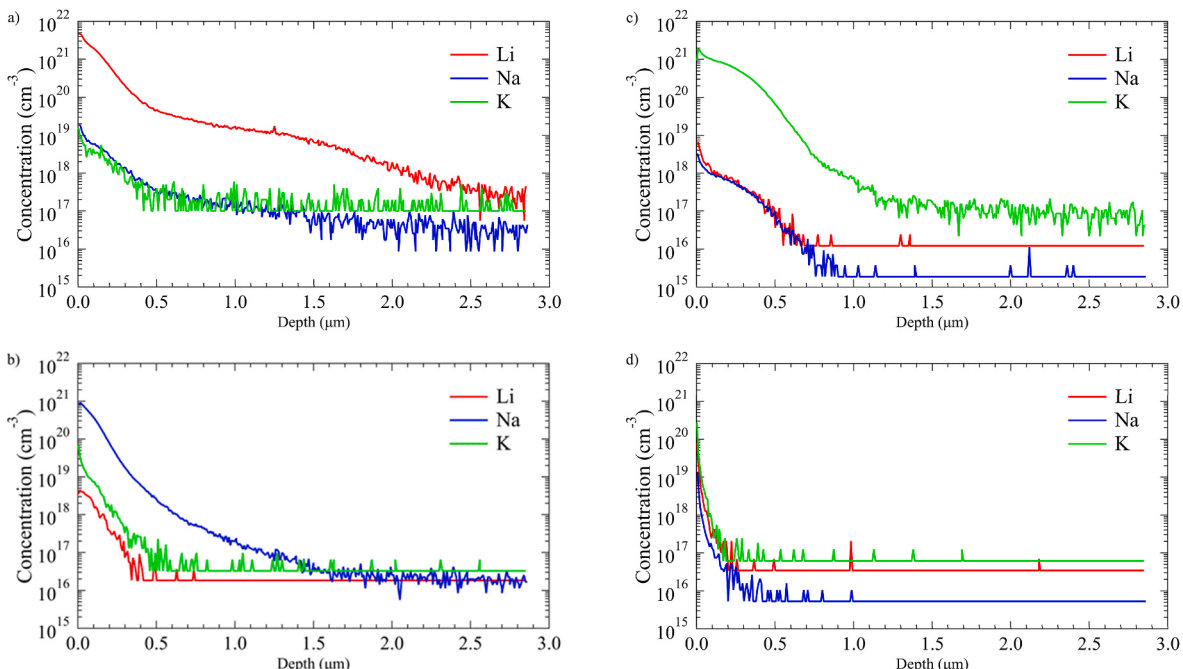


Fig. 9. SIMS profiles after the PID tests of L2 module (after 96 h PID test) a), N1 module (after 96 h PID test) b), K2 module (after 72 h PID test) c), and H module (after 72 h PID test) d).

4. Conclusions

In this study, we carried out the PID and the anneal tests on modules without cover glass using c-Si solar cells contaminated with aqueous chloride solutions of different alkali metal elements. It was found that in the presence of a potential difference between the solar cell and the module surface, all alkali metal elements penetrate the solar cell due to the electric field applied during the PID test. Furthermore, only Na element specifically caused the PID-s phenomenon, while other alkali metal elements do not cause distinct PID-s phenomenon. Moreover, it was suggested that the Li element may mitigate the PID-s phenomenon caused by Na element. Our work enriches the understanding of the PID-s phenomena and presents the possibility of utilizing a small amount of Li element on the solar cell surface to prevent the PID-s phenomenon.

CRediT authorship contribution statement

Yiming Qin: Writing – original draft, Formal analysis, Data curation. **Asahi Yonemoto:** Writing – review & editing, Validation, Investigation, Formal analysis. **Marwan Dhamrin:** Writing – review & editing, Resources. **Keisuke Ohdaira:** Writing – review & editing, Resources. **Kazuhiro Gotoh:** Writing – review & editing, Supervision, Conceptualization. **Atsushi Masuda:** Writing – review & editing, Supervision.

Declaration of competing interest

The authors declare the following financial interests/personal relationships which may be considered as potential competing interests: Yiming Qin reports financial support was provided by JST SPRING. If there are other authors, they declare that they have no known competing financial interests or personal relationships that could have appeared to influence the work reported in this paper.

Acknowledgment

This work was supported by JST SPRING, Grant Number JPMJSP2121.

Data availability

Data will be made available on request.

References

- [1] S. Pingel, O. Frank, M. Winkler, S. Daryan, T. Geipel, H. Hoehne, J. Berghold, Potential induced degradation of solar cells and panels, in: Proceedings of the 35th IEEE Photovoltaic Specialists Conference, June 20–25, 2010, pp. 2817–2822, <https://doi.org/10.1109/PVSC.2010.5616823>. Honolulu, HI, USA.
- [2] P. Hacke, M. Kempe, K. Terwilliger, S. Glick, N. Call, S. Johnston, S. Kurtz, I. Bennett, M. Kloos, Characterization of multicrystalline silicon modules with system bias voltage applied in damp heat, in: Proceedings of the 25th European Photovoltaic Solar Energy Conference and Exhibition and the 5th World Conference on Photovoltaic Energy Conversion, September 6–10, 2010, pp. 3760–3765, <https://doi.org/10.4229/25thEUPVSEC2010-4BO.9.6>. Valencia, Spain.
- [3] P. Hacke, K. Terwilliger, R. Smith, S. Glick, J. Pankow, M. Kempe, S. Kurtz, I. Bennet, M. Kloss, System voltage potential-induced degradation mechanisms in PV modules and methods for test, in: Proceedings of the 37th IEEE Photovoltaic Specialists Conference, June 19–24, 2011, pp. 814–820, <https://doi.org/10.1109/PVSC.2011.6186079>. Seattle, WA, USA.
- [4] H. Nagel, A. Metz, K. Wangemann, Crystalline Si solar cells and modules featuring excellent stability against potential-induced degradation, in: Proceedings of the 26th European Photovoltaic Solar Energy Conference and Exhibition, September 5–9, 2011, pp. 3107–3112, <https://doi.org/10.4229/26thEUPVSEC2011-4CO.5.6>. Hamburg, Germany.
- [5] V. Naumann, D. Lausch, A. Hähnel, J. Bauer, O. Breitenstein, A. Graff, M. Werner, S. Swatek, S. Großer, J. Bagdahn, C. Hagendorf, Explanation of potential-induced degradation of the shunting type by Na decoration of stacking faults in Si solar cells, Sol. Energy Mater. Sol. Cell. 120 (A) (2014) 383–389, <https://doi.org/10.1016/j.solmat.2013.06.015>.
- [6] C. Taubitz, M. Schütze, M.B. Koentopp, Towards a kinetic model of potential-induced shunting, in: Proceedings of the 27th European Photovoltaic Solar Energy Conference and Exhibition, September 24–28, 2012, pp. 3172–3176, <https://doi.org/10.4229/27thEUPVSEC2012-4DO.6.6>. Frankfurt, Germany.
- [7] D. Lausch, V. Naumann, O. Breitenstein, J. Bauer, A. Graff, J. Bagdahn, C. Hagendorf, Potential-induced degradation (PID): introduction of a novel test approach and explanation of increased depletion region recombination, IEEE J. Photovoltaics 4 (3) (2014) 834–840, <https://doi.org/10.1109/JPHOTOV.2014.2300238>.
- [8] V. Naumann, D. Lausch, C. Hagendorf, Sodium decoration of PID-s crystal defects after corona induced degradation of bare silicon solar cells, Energy Proc. 77 (2015) 397–401, <https://doi.org/10.1016/j.egypro.2015.07.055>.
- [9] S. Jonai, A. Masuda, Origin of Na causing potential-induced degradation for P-type crystalline Si photovoltaic modules, AIP Adv. 8 (11) (2018) 115311, <https://doi.org/10.1063/1.5040516>.
- [10] Photovoltaic (PV), Modules –Test Methods for the Detection of Potential-Induced Degradation– Part 1: Crystalline Silicon, IEC TS 62804-1, International Electrotechnical Commission, 2015.
- [11] K. Hara, H. Ichinose, T.N. Murakami, A. Masuda, Crystalline Si photovoltaic modules based on TiO₂-coated cover glass against potential-induced degradation, RSC Adv. 4 (2014) 44291–44295, <https://doi.org/10.1039/c4ra06791f>.
- [12] J. Berghold, P. Grunow, P. Hacke, W. Hermann, S. Hoffmann, S. Janke, B. Jaeckel, S. Koch, M. Koehl, G. Mathiak, et al., PID test round robins and outdoor correlation, in: Proceedings of the 28th European Photovoltaic Solar Energy Conference and Exhibition, 2013, pp. 3003–3011, <https://doi.org/10.4229/28thEUPVSEC2013-4DO.3.4>. September 30–October 4, Paris, France.
- [13] S. Yamaguchi, K. Ohdaira, Degradation behavior of crystalline silicon solar cells in a cell-level potential-induced degradation test, Sol. Energy 155 (2017) 739–744, <https://doi.org/10.1016/j.solener.2017.07.009>.
- [14] J. Slamberger, M. Schwark, B. B Van Aken, P. Virtič, Comparison of potential-induced degradation (PID) of N-type and P-type silicon solar cells, Energy 161 (2018) 266–276, <https://doi.org/10.1016/j.energy.2018.07.118>.
- [15] W. Luo, P. Hacke, K. Terwilliger, T.S. Liang, Y. Wang, S. Ramakrishna, A.G. Aberle, Y.S. Khoo, Elucidating potential-induced degradation in bifacial PERC silicon photovoltaic modules, Prog. Photovoltaics Res. Appl. 26 (10) (2018) 859–867, <https://doi.org/10.1002/pip.3028>.
- [16] W. Luo, P. Hacke, S.M. Hsian, Y. Wang, A.G. Aberle, S. Ramakrishna, Y.S. Khoo, Investigation of the impact of illumination on the polarization-type potential-induced degradation of crystalline silicon photovoltaic modules, IEEE J. Photovoltaics 8 (5) (2018) 1168–1173, <https://doi.org/10.1109/JPHOTOV.2018.2843791>.
- [17] J. Carolus, J.A. Tsanakas, A. van der Heide, E. Voroshazi, W.D. Ceuninck, M. Daenen, Physics of potential-induced degradation in bifacial p-PERC solar cells, Sol. Energy Mater. Sol. Cells 200 (2019) 109950, <https://doi.org/10.1016/j.solmat.2019.109950>.
- [18] K. Sporleder, V. Naumann, J. Bauer, S. Richter, A. Hähnel, S. Großer, M. Turek, C. Hagendorf, Local corrosion of silicon as root cause for potential-induced degradation at the rear side of bifacial PERC solar cells, Phys. Status Solidi Rapid Res. Lett. 13 (9) (2019) 1900163, <https://doi.org/10.1002/pssr.201900163>.
- [19] K. Sporleder, V. Naumann, J. Bauer, S. Richter, A. Hähnel, S. Großer, M. Turek, C. Hagendorf, Root cause analysis on corrosive potential-induced degradation effects at the rear side of bifacial silicon PERC solar cells, Sol. Energy Mater. Sol. Cell. 201 (2019) 110062, <https://doi.org/10.1016/j.solmat.2019.110062>.
- [20] K. Sporleder, V. Naumann, J. Bauer, S. Richter, A. Hähnel, S. Großer, M. Turek, C. Hagendorf, Microstructural analysis of local silicon corrosion of bifacial solar cells as root cause of potential-induced degradation at the rear side, Physica Status Solidi (A) App. Materials Sci. 216 (17) (2019) 1900334, <https://doi.org/10.1002/pssa.201900334>.
- [21] K. Sporleder, J. Bauer, S. Großer, S. Richter, A. Hähnel, M. Turek, V. Naumann, K. Ilse, C. Hagendorf, Potential-induced degradation of bifacial PERC solar cells under illumination, IEEE J. Photovoltaics 9 (6) (2019) 1522–1525, <https://doi.org/10.1109/JPHOTOV.2019.2937231>.
- [22] K. Fujita, Y. Takahara, Y. Chikaura, Influence of refining agent in soda lime glass for ultraviolet ray transmittance, Mater. Trans. 49 (2) (2008) 372–375, <https://doi.org/10.2320/matertrans.MRA2007172>.
- [23] S. Jonai, Y. Tachibana, K. Nakamura, Y. Ishikawa, Y. Uraoka, A. Masuda, Roles of SiN_x in potential-induced degradation for P-type crystalline Si photovoltaic modules, in: Proceedings of the 46th IEEE Photovoltaic Specialists Conference, June 16–21, 2019, pp. 1969–1971, <https://doi.org/10.1109/pvsc40753.2019.8980826>. Chicago, IL, USA.
- [24] X. Li, Y. Yang, K. Jiang, S. Huang, W. Zhao, Z. Li, G. Wang, A. Han, J. Yu, D. Li, et al., Potential-free sodium-induced degradation of silicon heterojunction solar cells, Prog. Photovoltaics Res. Appl. 31 (9) (2023) 939–948, <https://doi.org/10.1002/pip.3698>.
- [25] S.P. Harvey, J.A. Aguiar, P. Hacke, H. Guthrey, S. Johnston, M. Al-Jassim, Sodium accumulation at potential-induced degradation shunted areas in polycrystalline silicon modules, IEEE J. Photovoltaics 6 (6) (2016) 1440–1445, <https://doi.org/10.1109/JPHOTOV.2016.2601950>.

- [26] Y. Komatsu, S. Yamaguchi, A. Masuda, K. Ohdaira, Multistage performance deterioration in N-type crystalline silicon photovoltaic modules undergoing potential-induced degradation, *Microelectron. Reliab.* 84 (2018) 127–133, <https://doi.org/10.1016/j.micrel.2018.03.018>.
- [27] S. Steingrube, O. Breitenstein, K. Ramspeck, S. Glunz, A. Schenk, P.P. Altermatt, Explanation of commonly observed shunt currents in c-Si solar cells by means of recombination statistics beyond the shockley-read-Hall approximation, *J. Appl. Phys.* 110 (1) (2011) 014515, <https://doi.org/10.1063/1.3607310>.
- [28] V. Naumann, C. Brzuska, M. Werner, S. Großer, C. Hagendorf, Investigations on the formation of stacking fault-like PID-shunts, *Energy Proc.* 92 (2016) 569–575, <https://doi.org/10.1016/j.egypro.2016.07.021>.
- [29] D. Yu, W. Cao, H. Wu, J. Zhao, Ionic radius scale of establishing synthesis factor of ionic mass and electricity, *Acta Phys. Chim. Sin.* 23 (5) (2007) 683–687, [https://doi.org/10.1016/S1872-1508\(07\)60043-6](https://doi.org/10.1016/S1872-1508(07)60043-6).
- [30] S. M. Sze, K.K. Ng, “Physics of Semiconductor Devices” third ed. (Wiley) p. 2S3.